Carbonates and Evaporites (2021) 36:74
https://doi.org/10.1007/s13146-021-00724-7

ORIGINAL ARTICLE

Expansion and sea-level change of paleocanyon Seymareh Member (*Lopha* limestone), Zagros, and Iran

Afshin Hashmie[1] · Neda Ghotbi[2] · Samira Sharyari[3] · Samira Rahimi[4]

Accepted: 5 July 2021 / Published online: 16 August 2021

Abstract

This study is made clear expansion, depositional architecture, and sea-level change of the Seymareh Member. The Campanian carbonate sequence (Seymareh Member) of the Lurestan Zone, contains a rich macrofauna. Amid the bivalves, oysters (*Lopha* sp.) and echnoids are abundant and are mostly well conserved, in some beds dominating the fauna. Rich fossiliferous strata of Seymareh Member are 10–300 m and widespread in the south Lurestan Zone. A submarine canyon in the shelf is suggested for the depositional environment of the Seymareh Member which deepens to the east (Anaran and Surgah, Emam-Hasan anticline) and thins in west locations (Pasan, Soltan and Kabir-Kuh anticline). This present study is novel because few papers provide a complete overview of the frequency Seymareh canyons and out into deep water basins. The paleocanyon deposits conserved south Lurestan Zone provide an occasion for extending sequence stratigraphic ideas and thought associated with submarine canyons and deep-sea deposits. The Seymareh Member were deposited at a more toward the sea situated continental slope or outer belt region of the Late Cretaceous upwelling system and 4th order cyclic sequences in the Seymareh Member are recognised. Below these lowstand conditions, oyster shells were poured off the bioherms and deposited as large cross-bedded units on the flanks of the basins. At the same time, antecedent glauconite and phosphatic deposits were reworked and winnowed to form high-grade phosphorite.

Keywords Seymareh Member · Lopha · Depositional environment · Campanian · Lurestan zone · Zagros

Introduction

Ocean margins Late Cretacoues are vigorous environments which host costly deep-water benthic ecosystems. In the Campanian, a prosperous shoal of oyster, echinoid spines, gastropod and foraminifera increased briefly from Northeast Iraq and Southeast Turkey (Aqra and Tayarat Formation) (Jassim and Goff 2006; Karim and Surdashy 2005) into western Lurestan Zone and manufacture the shell bed (Seymareh Member) of the Gurpi Formation. Seymareh (Lopha) Member from the Gurpi Formation are well exposed in the southwest Lutestan Zone in Zagros basin, with a high sedimentation appraise. The Seymareh (Lopha) Member name is extracted from the abundance of Lopha shells and Seymareh River in Plangane anticline in Lurestan Zone. In every part of the Seymareh Member, many groups of organisms evolved and utilized considerably different biological procedures to form carbonate advancement with unique constitutions. All micropalaeontologists have faith that the Gurpi Formation has individual ages based on Foraminifera and Nannofossil studies in individual localities in the Zagros basin and a few detailed investigations on Seymareh Member have been attempted (Hashemi et al. 2020; Zarei and Ghasemi-Nejad 2014; Balmaki et al. 2010 (in Persian)), however, detailed sedimentological, stratigraphy and facies work in Seymareh Member is still required. No previous work has been executed on the expansion and sea-level change of Seymareh Member of this time interval. The general, purpose of this paper is to evaluate paleo-environments, sea-level change and expansion of the Seymareh Member of the Gurpi Formation in the southwest Lurestan Zone (Ahmad et al. 2015: Ayoub-Hannaa

✉ Afshin Hashmie
Hashmieafshin@gmail.com

[1] Independent Researcher, Graduated from Sedimentology, Shiraz, Iran

[2] Department of Geology, Faculty of Earth Sciences, Shiraz University, Shiraz, Iran

[3] Department of Geology, Faculty of Earth Science, Shahid Beheshti University, Tehran, Iran

[4] Department of Geology, Faculty of Sciences, Ferdowsi University of Mashhad, Mashhad, Iran

and Fürsich 2011; Barrera and Savin 1999; Beiranvand et al. 2013; Burst 1958; Casini et al. 2011; Darabi and Sadeghi 2017; Darabi et al. 2018; Dill Jafar Nejad 2007; El-Sabbagh and Hedeny 2016; El-Sabbagh et al. 2015; Esmaeilbeig 2018; Geel 2000; Ghasemi-Nejad et al. 2006; Hadavi and Senemari 2010; Hower and Brown 1961; Hu et al. 2012; Jassim and Goff 2006; Mahanipour and Najafpour 2016; Malchus 1998; Mekawy 2013; Nairn and Alsharhan 1997; Najafpour et al. 2015; Okan and Hoşgör 2010; Razmjooei et al. 2014, 2018; Senemari and Usefi 2013; Sharyari et al. 2018; Wagner and Benndorf 2007; Zakhera et al. 2017) are used in this paper.

Geological setting, material and methods

The breach of Arabia (also Zagros basin) from Africa and its coming together with Eurasia was the last in a series of separation-collision events which bestow stand up to the Alpine-Himalayan orogenic system (Farzipour-Saein et al. 2009). The Zagros Mountains act of stretching over the different area (Fig. 1a), and the Seymareh Member comprises within the basin cropping out widely in southwest Lurestan Zone (Zarei and Ghasemi-Nejad 2014) (Fig. 1b). In Lurestan, the belt is bounded in the NE by the Main Zagros reverse fault and main recent fault (Fig. 1b). The Bala Rud Fault (or line) segregate the eastern Lurestan zone from the Dezful Embaymen (Hessami et al. 2001; Blanc et al. 2003) and the west, Lurestan is bounded by the Khaneqin fault which segregate it from the Kirkuk Embayment and the northeast-southwest the Lurestan zone is bounded by the High Zagros Fault, from the southwest by the Mountain (Fig. 1b). Gurpi Formation is a deposit of the following Zagros time that is one of the great source rocks of oil in Iran; (Motiei 1993; Darvishzadeh 2009). In this study, nine stratigraphic sections (Anticline) of the Seymareh Member have been selected, measured and sampled in the SW and central Lurestan zone (Fig. 1b). So that from the east to west, they include, south and north flank Kabir-Kuh (two section), Samand, Kasseh-mast, Anaran, Surgah, Anjir, Tang-e-bijar and Emam-hassan anticlines (Fig. 2). Satellite picture and panoramic photo-mosaic were usual for line-drawing of succession architecture, key bounding surfaces and bedding model. Field observations were complemented with the study of 97 thin-sections for textural characterization and recognition of skeletal components. Some samples have been analysed to make certain about glauconites, quartz, and iron and phosphorite contents. The combined use of facies and sedimentologic

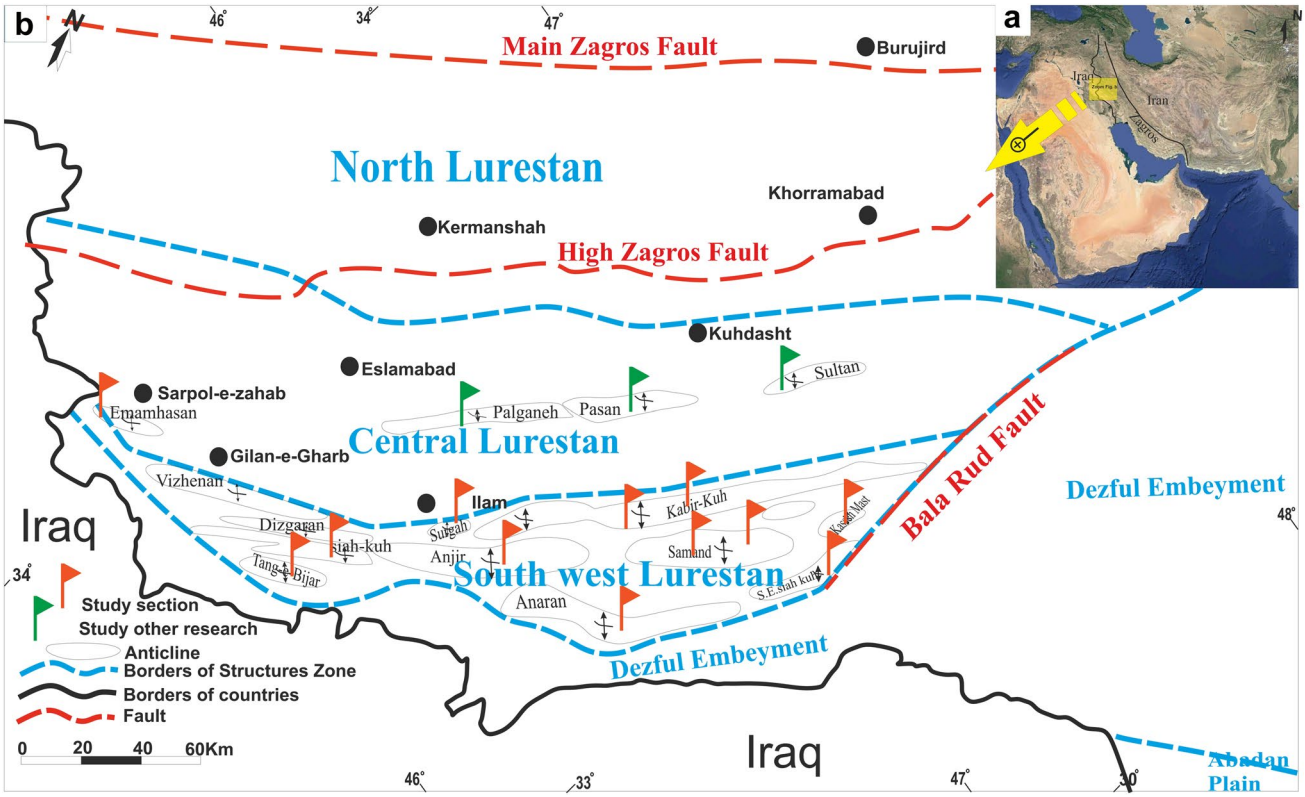

Fig. 1 **a** Location map of Iran and geological provinces of the Zagros Mountains. The rectangle indicates the study area, **b** close-up view of a yellow rectangle of **a**. Map of present-day of Zagros showing the geographical domains as well as the main sutures and tectonic structures (modified from Homke et al. 2009; Sherkati et al. 2005) locations of measured sections

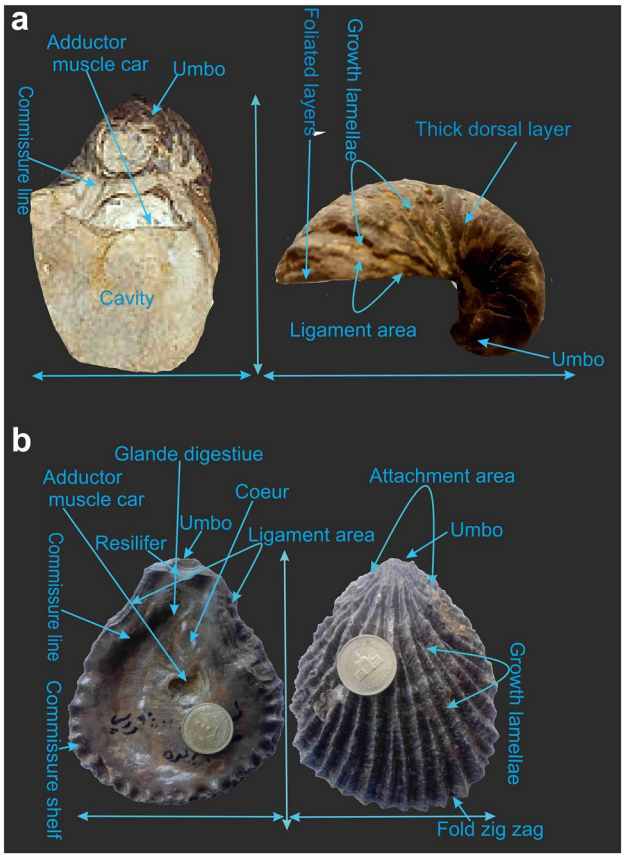

Fig. 2 **a** Gross anatomy of *Pycnodonte* in Seymareh Member. **b** Summary diagram showing morphologhy and measurements of *Lopha* shells in south flank Kabir-Kuh section

features (e.g. grain size, degree of sorting, grain composition and sedimentary structures) has resulted in high-resolution correlations for the Seymareh Member across the sections depression and supply a framework for the explanation of a detailed depositional environment and sea-level change.

Lopha sp. in Seymareh Member

Lopha are classified mainly on the basis of their interior and exterior shell nature and, in some cases, shell microstructure. Significant internal characters are the shape of the ligament area, the umbonal cavity, the outline and position of the rear adductor muscle scar, and the type and attendance of Seymareh Member. Exterior characters include size, the general outline of the shell, the tendency and type of coiling of the umbo, the shape and development of the attachment area (Fig. 2), and shell decoration such as concentric growth lines, radial ribs, folds, nodes and spines (Stenzel 1971; Malchus 1996; Aqrabawi 1993; Checa and Jiménez-Jiménez 2003). In contrast, nearly all larger specimens, mainly of *Pycnodonte* sp., *Pycnodonta vesicularis, Lopha dichotoma* and *Lopha* sp. are preserved unbroken and intelligible. This show transport under high-energy situation, but of short duration, as abrasion and breakage are usually low. Ribbed Lopha of the Seymareh Member lineage could have originated in the study area during the Late Campanian in the warm (e.g.: Aqrabawi 1993), ventilated, nutrient-rich, near-shore waters of the Late Cretaceous Seaway. This *Lopha* Sp. is a simple ribbed oyster built on a generalized plan that could be the ancestor of the smaller, younger, inequivalved species of *Pycnodonte* mentioned above. At maturity, these plications thicken into prongs that form the steep flanks of the shell (Seymareh Member). These prongs create an interlocking, zigzag commissure (Fig. 2). Left valves are often attached to the right valves of other individuals of the species. Therefore, the plications are commonly more noticeable on the right valves. The amplitude of the prongs decreases in the opposite direction toward the umbo, where the amplitudes of the prongs are suppressed completely. This would minimize the extra resistance to the flow of water through the gape, caused by drag against the lengthened edges of the valves. Any zigzag must be a compromise between protection and rate of flow." Zigzag commissures provide protection by acting as straining devices while the valves are open. The zigzag slit allows particles below a critical size (diameter) to enter the mantle cavity but rejects particles greater than that critical diameter. In addition to its protective function on *Lopha* sp., the onset of the zigzag commissure, which does not appear until late in the growth cycle of the oyster, allows the oyster to grow larger by increasing the interior volume of the shell. Crowding may have been as big a trigger for flank growth as maturity. The ridges of the oyster flanks that resulted from thickening the costae (ribs) into prongs may have increased the strength of the shell as well. *Pycnodonte* and *Lopha* species occur in abundance and attain large size in Lopha Member, where they occur together in the same bed and, thus, occur in the same paleoenvironment. *Lopha* sp. and *Pycnodonte* are found in each of the rock units in different sizes.

Lithostratigraphy and widespread Seymareh Member

Seymareh Member has been deposited only in Lurestan with great changes in thickness, facies (Fig. 3). The Seymareh Member is known as Lopha limestone, due to its abundance of macrofaunal (especially Lopha fossil). According to research by Hashmie et al. (2020) Seymareh Member is composed of four stratigraphic units that do not appear anywhere. Sina et al. (2010) and Darabi et al. (2017) have reported the fossil debris Lopha in Pasan and Sultan anticline, but have incompletely reported the sequence of the Seymareh Member. The first and

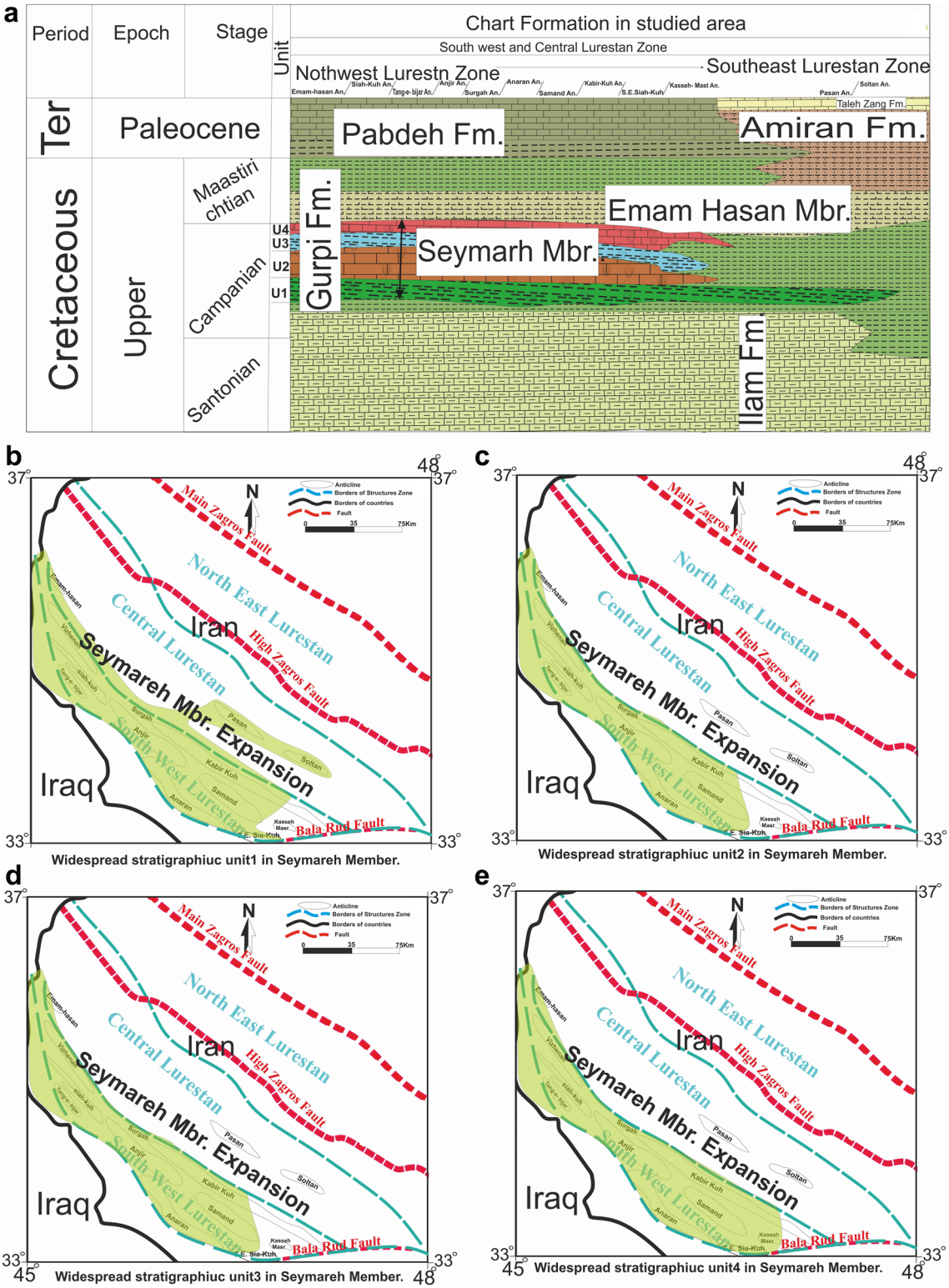

Fig. 3 **a** Stratigraphic nomenclature for the Seymareh Member in the studied sections (with slightly modified after Motiei 1995). **b** Widespread stratigraphic unit 1 in Seymareh Member of Lurestan Zone. **c** Widespread stratigraphic unit 2 in seymareh Member of Lurestan Zone during the late Campanian–Maastrichtian. **d** Widespread stratigraphic unit 3 in seymareh Member of Lurestan Zone. **e** Widespread stratigraphic unit 2 in Seymareh Member of Lurestan Zone during the Campanian-Maastrichtian

third stratigraphic units are erosive due to the nature of shale form, but the second and fourth stratigraphic units are usually prominent and separable. The percentage of *Lopha* sp., as shown in Fig. 3, increases from unit 1 to unit 2 and then decreases again to Unit 4. The percentage of organisms was averaged from all sections. In general, the percentage of *Lopha* sp. and other macrofossil from the northeast to the southwest of Lurestan zone decreases, so that the percentage in Kabir-Kuh section is decreased to the Emam-hasan section (Fig. 3). Three additional sections measured other researcher has also been used to better understand the depositional architecture across the basin. In the platform-to-basin transition, from SE (Soltan) to NW (Emam-hasan anticline) in the southwest and central Lurestan zone, the stratal architecture and distribution of allochem allow four large-scale stratigraphic units to be distinguished (Fig. 4). According to previous studies and this study, Seymareh Member is more widespread in the southwest of Lurestan and in the southern regions of central Lurestan Zone and is not observed in other areas of the Zagros basin. Figure 4 shows the extent of Seymareh Member expansion and Fig. 3 shows the distribution of each stratigraphic units in Lurestan province. Stratigraphic Unit 1 is observed in the central and southwestern Lurestan Zone with different thickness (Fig. 4a). The stratigraphic units2 and 3 are observed in the southwestern Lurestan Zone and always together (Fig. 4b and c). The stratigraphic unit4 is observed in the southwest Lurestan Zone (Fig. 4d).

Biostratigraphy and facies

The biostratigraphic criteria of the Seymareh Member more were established by foraminifers and calcareous nannofossils. It should be noted that the beginning and end of the Seymareh

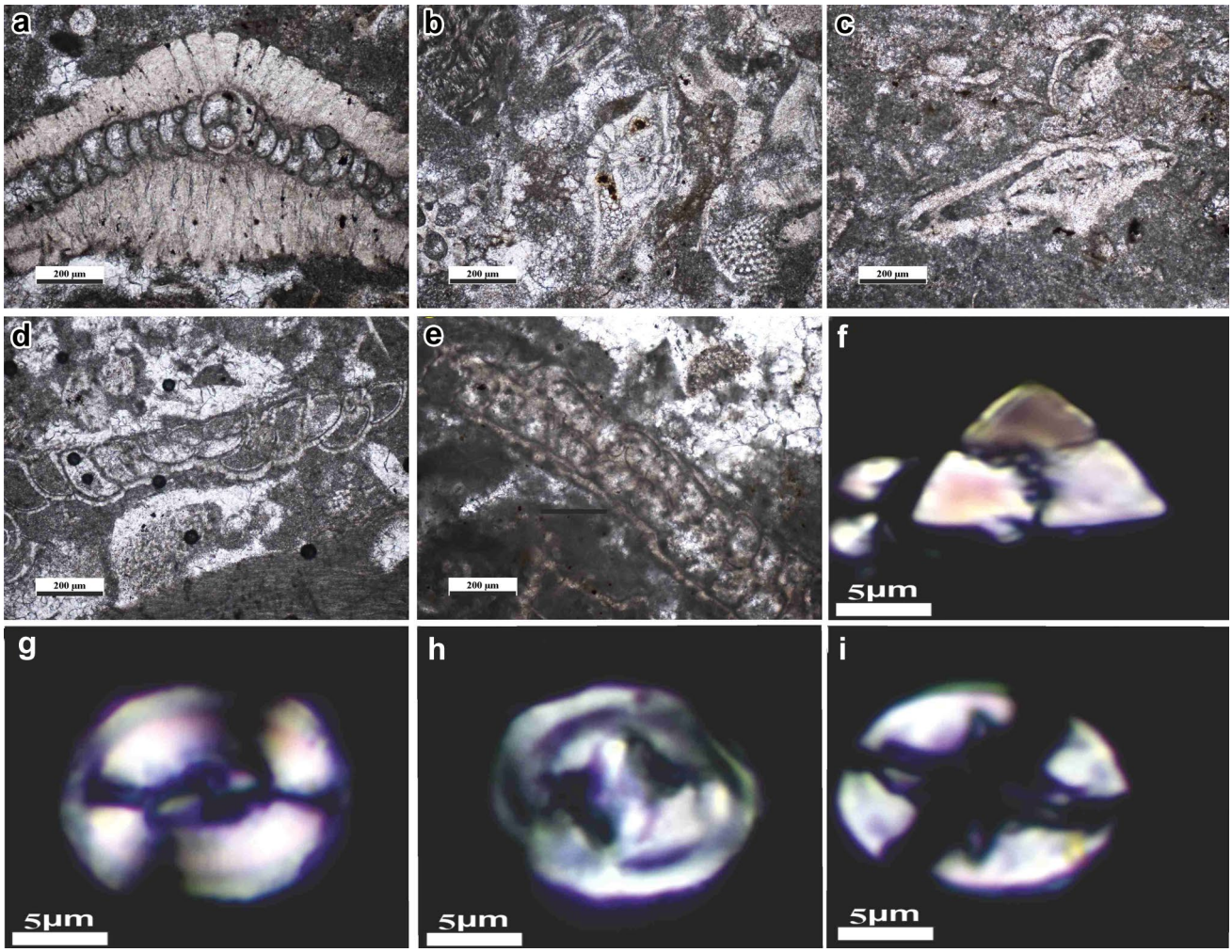

Fig. 4 Photomicrographs showing: **a** *Orbitoides* sp. in South flank Kabir-Kuh section. **b** *Sirtina orbitoidesformis* in north flank Kabir-Kuh section. **c** *Goupillaudina iranica* in Anaran section. **d** *Planorbulina* sp. in Emam-hasan section. **e** *Omphalocyclus macroprus* Anjir section. **f** *U. trifidus*-short ray nano fossil in Samand section. **g** *B. parca constrita* in Surgah section. **h** *R. levis* in Anaran section. **i** *E. eximius* in Anaran section

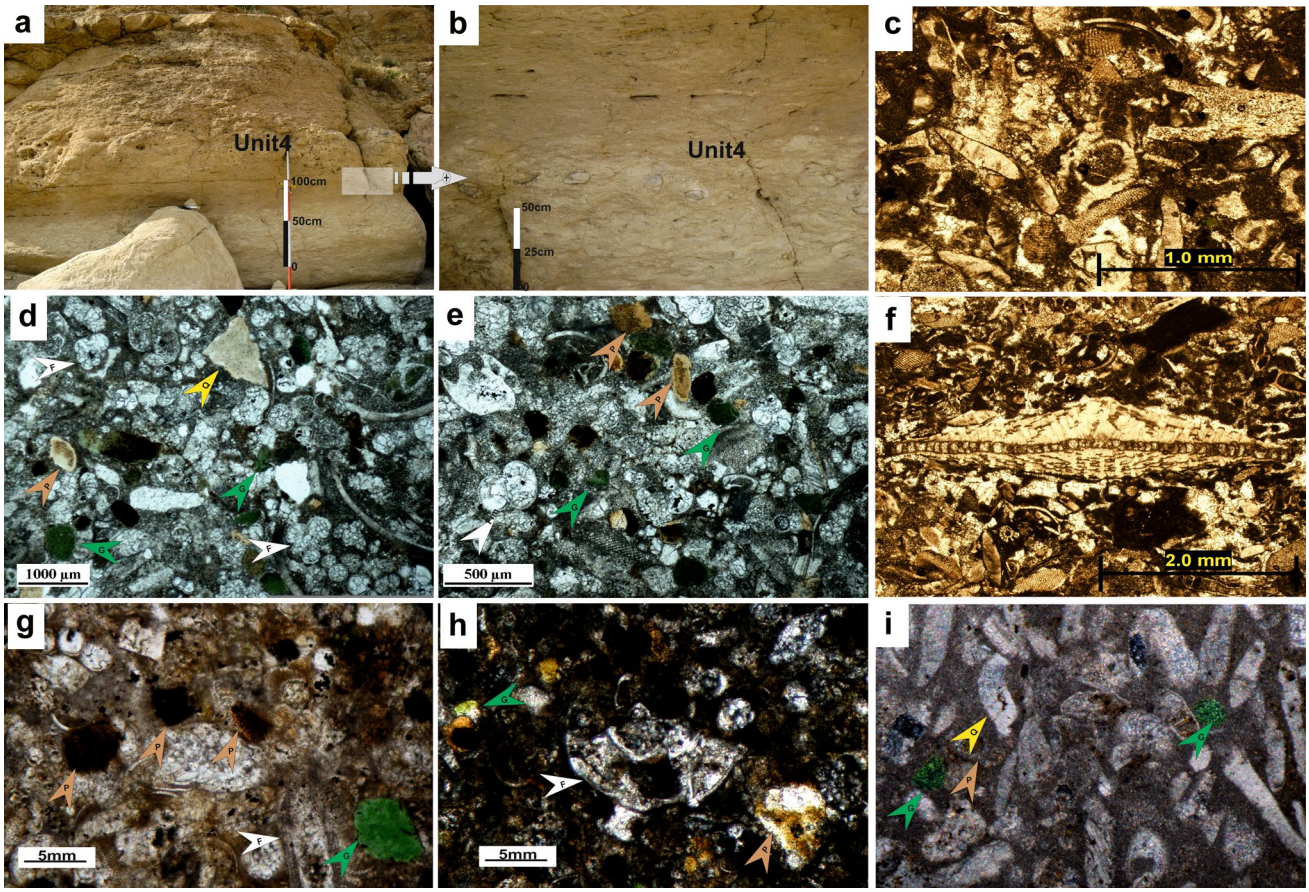

Fig. 5 Field photographs and microscope of the Seymareh Member successions of the studied sections. **a** Stratigraphic unit 4 in Anaran section. **b** Close-up view of grey square of Fig. an in unit 4 in Anaran in section. **c** Lopha-benthic forams floatstone-rudstone microfacies with fossil debris in unit 4 in Anaran anticline. **d** Foraminifera bioclastic wackestone/packstone microfacies with glauconite, phosphate, quartz grains and foraminifera in unit 4 in Emam-hasan section. **e** Foraminifera bioclastic wackestone/packstone microfacies with glauconite and phosphate and quartz grains and foraminifera in unit 4 in Samand section. **f** Lopha-benthic forams floatstone-rudstone microfacies with fossil debris in unit 2 in Kase-Mast anticline. **g** Shelly oyster wackestone microfacies with glauconite and phosphate grains in unit3 in south flank Kabir-kuh section **h** Shelly oyster wackestone microfacies with glauconite and phosphate grains in unit 2 in south flank Kabir-kuh section. **i** Foraminifera bioclastic wackestone/packstone microfacies with glauconite and phosphate and quartz grains and foraminifera in unit4 in Emam-hasan anticline section. *F* foraminifera, *Q* quartz, *G* glaconite, *P* phosphate

Member have been identified in sequence with the appearance of *Lopha* sp. fossil. Numerous biostratigraphic studies performed in this area by various research institutes and investigators on foraminifers and calcareous nannofossils groups (e.g. Sharyari et al. 2017; Rahimi et al. 2017, 2020) have estimated the age of Seymareh Member equal Late Campanian-Early Maastrichtian by using foraminifers and calcareous nannofossils in Kabirkuh, Samand and Anaran sections (Fig. 5). By using calcareous nannofossils and foraminifers in both flank Kabir-Kuh anticline Hadavi and Rasa Ezadi (2008), Rabbani et al. (2009), Moradi (2010) and Rahimi et al. (2018, 2020) have estimated the age of Seymareh Member equal to Late Campanian. Hemmati-Nasab et al. (2008), Zarei and Ghasemi-Nejad (2014) using foraminifers and Sharyari et al. (2017) by calcareous nannofossils in Anaran anticline have appraise the age of Saymareh Member equal Late Campanian and another studied research brief: Hadavi and Shokri (2010), Sina et al. (2010), Bakhshandeh et al. (2015), Darabi et al. (2017). The Seymare Member consists of a large variety of skeletal and non-skeletal grains, iron, glauconite and phosphatic grain and sparite and micrite cement. Differences in the abundance of allochems exist between all study sections. Non-skeletal grains are abundant in all sections and consist mainly of glauconite, quartz, and interclast grains. Skeletal grains are mostly oyster (Lopha), bivalves, gastropods, echnoids, bryozoer and benthic and pllagic foraminifers. Therefore, several significant taphonomic processes were affecting the shells and changing their original state during fossilization. The principal depositional features observed in the field and thin-sections, such as textures and microfossils, arrives in the identification of distinctive facies microfacies in all sections (Table 1, Figs. 5 and 6).

Table 1 Major facies and paleoenvirnment of the stratigraphic units in Seymareh Member. Modified after Hashmie et al. 2020

Facies	Unit place	Paleoenvirnment
Shelly oyster intraclast grainstone	Unit 1 and 3	Upper Canyon
Shelly oyster wackestone	Unit 1	Lower Canyon to basin plain
Lopha-benthic forams floatstone-rudstone	Unit 2 and 4	Upper to middle canyon
Foraminifera bioclastic wackestone/packstone	Unit 1, 3 and 4	Middle to lower canyon

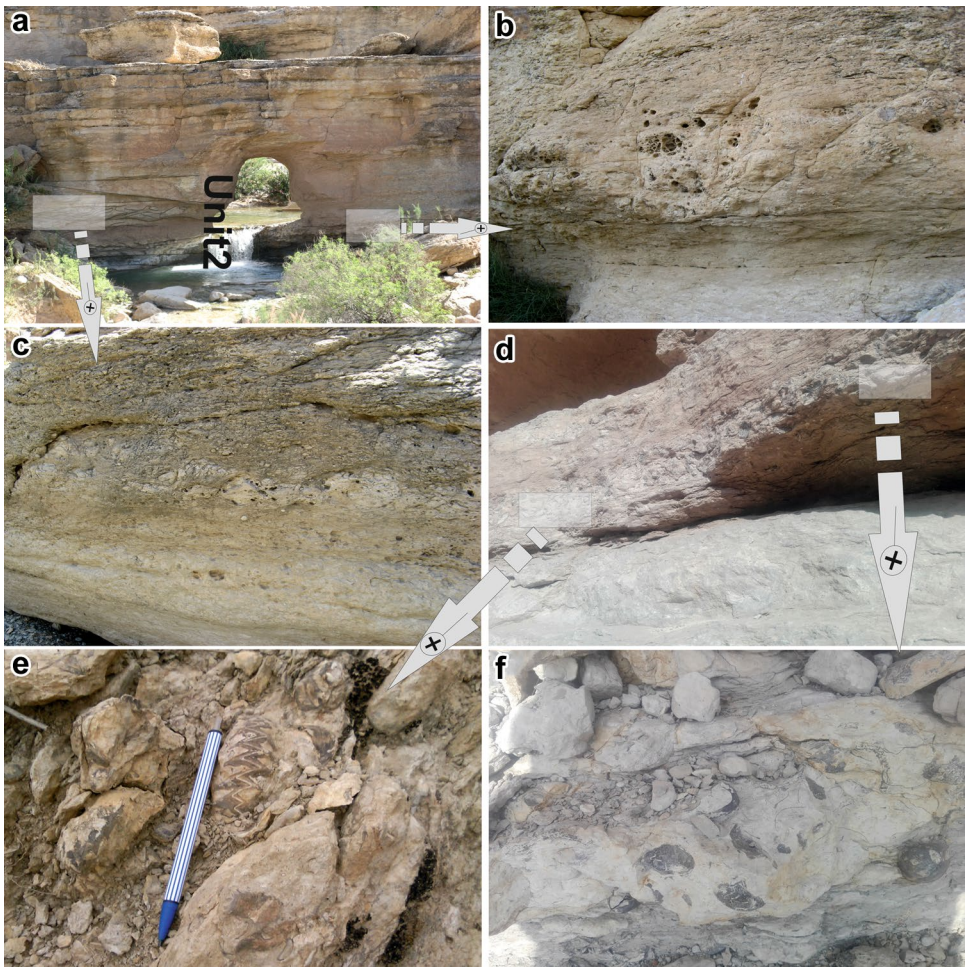

Fig. 6 **a** Field photographs of unit 2 of the Samand section. **b** Close-up view of grey square of **a** with cavity erosion. **c** Close-up view of grey square of **a** with convolute bedding and slump folding structures. **d** Outcrop photograph unit4 in Tan-e-bijar section. **e** Close-up view of grey square of **d** with *Lopha* sp. **f** Close-up view of grey square of **d** with *Pycnodonte* and *Lopha* sp

Whole-rock geochemistry

We demonstrate our results here and converse their connotation for water depth, paleoredox situations, and maturity. Thirty-two powdered glauconite samples were examined with XRF to determine the mineralogical constitution of the main part samples. The results of the XRF elemental abundances data of the main part thirty-two rock samples are listed in Table 2. These elements as identified from Table 2 are correlated well with glauconite as well as being themselves intercorrelated. The framework grains are composed mainly of glauconite grains with lesser amounts of fine- and rarely medium-grained quartz grains as well as phosphat. Glauconites are identified in all sections but are more abundant in the Kabir-Kuh anticline than in the Samand anticline in stratigraphic unit4. Most glauconites in the Seymareh Member are authigenic and alike in size, but in a few samples, they show sizable variation in size. They alter in colour from light green to lemon green in Seymareh Member. These frame grains were inclosed by a brownish marl and shale form matrix. In addition, glauconites grain is exited in other unit rock in Gurpi Formation (e.g.., Emam-Hassan Member). It is supposed that the small, similar-sized, well-sorted and alike-shaped in Seymareh Member are autochthonus which may show transportation before deposition. Some quartz was replaced by glauconites. Some glauconite grains look like foraminifer's shells. Apparently. these glauconites formed within foraminifera shells

Table 2 Major oxide values (wt. %) of the different unit's samples of the Seymareh Member in different stratigraphic units

Section	Place unit	Sample thickness (m)	SiO_2	Al_2O_3	BaO	CaO	Fe_2O_3	K_2O	MgO	MnO	Na_2O	P_2O_5	SO_3	TIO_2	LIO	
North crest Kabir-Kuh	1	20	18.1	9.8	1.5	39.9	12.3	1.5	2.6	0.35	0.47	1.2	2.8	0.98	8.5	100
South crest Kabir-Kuh	1	18	9.6	8.2	0.6	48.3	3.6	8.9	6.7	0.35	0.35	4.4	5.6	0.3	3.1	100
Samand	1	14	5.3	6.5	0.1	31.2	8.3	3.6	2.5	35	0.61	0.7	0.6	0.32	5.2	100
Anaran	1	38	7.9	6.2	0.8	45.9	16.2	8.2	6.1	1.2	0.021	0.1	0.8	1.2	5.3	100.001
Surgha	1	16	10.2	6.8	0.8	43.9	15.1	0.2	5.2	0.9	0.32	0.4	8.2	0.58	7.3	100
Anjir	1	9	9.3	9.6	0.9	46.04	13.9	4.1	3.2	0.78	0.85	0.8	3.6	0.49	6.4	100
Sia-Kuh	1	28	5.8	9.6	0.4	39.9	15.8	3.1	0.9	0.99	0.65	1.3	12.0	0.62	8.8	100.001
Tang-e-bijar	1	8	13.5	10.0	0.5	47.0	14.2	2.6	1.9	0.68	0.09	0.4	0.5	0.58	8.0	100
Emam Hasan	1	35	16.2	11.0	0.9	29.4	10.8	9.9	2.1	0.56	0.84	7.3	3.9	0.89	6.2	100
North crest Kabir-Kuh	2	52	32.2	5.2	0.1	17.3	8.1	14.1	3.9	0.328	0.636	9.5	0.9	0.276	7.3	100
South crest Kabir-Kuh	2	43	6.0	14.7	0.0	47.0	1.5	8.2	0.4	0.07	0.28	9.8	0.9	0.18	10.7	100
South crest Kabir-Kuh	2	42	26.9	6.8	0.8	18.2	9.8	9.0	5.1	0.438	0.75	17.2	0.9	0.322	4.3	100
Samand	2	54	36.1	8.4	0.2	14.3	6.5	13.0	6.5	0.548	0.8	9.0	1.0	0.368	3.2	100
Anaran	2	97	17.5	2.02	0.1	35.8	4.7	13.1	0.3	0.02	0.45	9.0	0.5	0.1	16.4	100
Surgha	2	28	25.2	10.2	0.5	24.2	6.8	9.8	4.1	0.12	0.47	7.5	0.3	0.2	10.6	100
Anjir	2	17	22.6	8.5	0.2	35.3	8.4	12.4	2.7	0.92	0.45	6.8	0.2	0.23	1.2	100
Sia-Kuh	2	86	18.7	12.1	0.4	22.2	6.6	14.5	6.2	0.13	0.85	8.8	0.4	0.52	8.6	100
Tang-e-bijar	2	26	19.6	10.2	0.7	25.2	8.5	15.2	3.8	0.23	0.65	9.6	0.3	0.32	5.6	100
Emam Hasan	2	15	20.1	5.6	0.6	28.5	5.9	17.5	0.7	0.35	0.98	9.2	0.5	0.54	9.6	100
North crest Kabir-Kuh	3	64	24.6	14.1	0.9	37.2	7.8	7.2	2.1	0.54	0.64	0.3	0.8	0.36	3.5	100
South crest Kabir-Kuh	3	52	32.1	9.8	0.9	34.2	8.8	5.6	3.2	0.48	0.84	0.5	0.3	0.95	2.2	100
Samand	3	56	19.2	8.9	0.6	41.1	14.2	5.6	1.4	0.82	0.48	0.3	0.2	0.79	6.3	100
Anaran	3	103	23.3	10.2	0.2	39.3	7.3	11.5	3.1	0.65	0.22	0.8	0.7	0.582	2.1	100.002
Surgha	3	34	18.8	8.7	0.5	39.5	14.4	8.9	5.1	0.74	0.48	0.7	0.2	0.32	1.5	100
North crest Kabir-Kuh	4	78	0.82	9.5	0.05	45.3	1.4	9.1	0.4	0.05	0.58	16.5	0.7	0.13	15.5	100
South crest Kabir-Kuh	4	54	20.3	4.5	0.8	28.6	7.4	16.1	0.3	0.43	0.42	11.2	1.0	0.33	8.6	100
Kasse-Masst	4	5	21.0	7.2	0.1	24.4	7.0	15.0	3.7	0.35	0.52	8.3	1.0	0.32	11.0	100
Samand	4	61	28.6	3.1	0.05	32.2	5.0	10.4	1.6	0.05	0.47	9.0	0.8	0.32	8.5	100.001
Anaran	4	208	31.2	6.4	0.1	22.1	7.2	8.1	3.2	0.243	0.572	10.6	0.8	0.253	8.9	100
Surgha	4	45	30.0	7.6	0.2	20.5	4.6	15.0	5.9	0.493	0.808	11.1	0.6	0.345	2.8	100
Tang-e-Bijar	4	31	35.7	16.0	0.1	12.3	8.7	11.1	4.5	0.383	0.693	3.4	0.9	0.299	5.8	100
Emam Hasan	4	33	14.2	12.2	0.4	41.3	7.4	11.4	4.4	0.48	0.5541	2.8	0.6	0.383	3.8	100.004

(Podobina and Kseneva 2005). A mixed study includes detailed petrography, mineralogy, and mineral chemical analysis (XRF) is likely to supply a better viewpoint of an agent touching the make-up of glauconite (Table 2). The remarkable variations in the chemistry of glauconites of the unusual studied areas could be ascribed to their distinction in the mineralogical component (pyrite goethite). However, authigenic glauconite may form in a wide spectrum of shallow marine environments involving wave-agitated estuaries and coastlines (Banerjee et al. 2016). Intraclasts are present in some samples of the Anaran, Kasse-mast, Samand, south flank of the Kabir-Kuh anticlines. Grain size quartz often is in the range of fine to medium (0.5–4 mm) that in most cases fine-grained sand-sized matrix fill between micrite. Grains are mostly bad-rounded quartz (Angular). The quartz grain is observed in the lower part Seymareh Member of fining upward cycles. Most intraclasts are in the interior homogenous and be composed of micrite, while others contain bioclasts. They are ordinarily polymodal in size ranging from 0.6 to 2.1 mm. Phosphate are not recognized in all sections. It comprises phosphate, quartz, and glauconite. Phosphate in all samples ranges from 0.01 to 0.3 mm (average 0.2 mm). It is supposed that the small, similar-sized, well-sorted, uniform-shaped and dark colored in 2 and 4 unite in Seymareh Member are debris grains, most grains were trapped by fossil debris. The results listed in Table 2 show more content of the average composition of SiO_2 (23.8 wt. %) at Seymarh Member contrasted to a variable component at the other vicinity. Al_2O_3 average composition displays variable content (7.6 wt. %) in the different localities with the higher values at Anaran, Samnd, Emam-hasan and Kabir-Kuh anticlines. Large variation in Fe_2O_3 average content (5.8 wt. %) in the analyse volume samples at the different localities were registered with the higher values at the north flank Kabir-Kuh anticline. K_2O average composition varies gently 11.4 wt. % in analyse volume samples of the different localities. The MgO average composition of glauconite (Table 1) varies 3.2 wt. %, with the higher values reported at all sections. On the other hand, the glauconites of both sections Kabir-Kuh samples exhibit more content in Al_2O_3 (t), K_2O, P_2O_5, whereas the glauconites of Anjir samples are comparatively enriched in P_2O_5 and SO_3. Contemporary glauconite forms in the depth range of 50–500 m and is most abundant between 200 and 300 m deep on the seafloor (Odin and Matter 1981). The Campanian-Maastrichtian border is at the end of stratigraphic unit 4. Before this border (beginning of Unit 4) to the beginning of Emam-Hassan Member, the amount of glauconite and phosphat has been increased. This shows that upwelling has really taken place on this border. In rock unit 1, the percentage of quartz is added from the beginning of Seymareh Member to rock unit 4 and this trend is observed in all studied sections. This trend shows that the depth of the Seymareh Member has decreased from the beginning to the top. Therefore, the amount of quartz has increased from the southeast of Lurestan zone (Kabirkuh sections) to the northwest of Lurestan zone (Imam Hassan section). The percentage of Al_2O_3 increases at the end of rock unit 1 (in all sections) and the beginning of rock unit 2. The above conditions indicate low environmental energy. The percentage of $Caco_3$ in all rock units is high. The percentage of Fe_2O_3 has increased from the end of rock unit 1 and the beginning of rock unit 2 and in narrow of Bijar, Siah Kuh, Anjir sections has increased in rock units 1 and in the middle of rock unit 3 the percentage of Fe_2O_3 in Samand and Surgah sections has increased. The amount of K_2O is directly related to the grains of gluconite, and wherever the grains of gluconite are increased, the amount of K_2O is also increased. In rock units 2 and 4, the concentration of gluconite is that this trend can be seen in almost all studied sections. The percentage of P_2O_5 in rock units 2 and 4 in the Anaran, Surgah, Kabirkuh sections has increased. It seems that the level of P_2O_5 and K_2O levels has reached the stage of sea-level change. The percentage of other elements was negligible. In general, it seems that rock units 2 and 4 have changed with environmental conditions and increasing living conditions, and phenomenon upwelling has occurred. This trend is observed in almost all studied sections. The climate during the Middle to Late Cretaceous (Aptian to Maastrichtian) practiced important changes from warm to colder periods with the highest sea surface temperatures in the Turonian (Friedrich et al. 2012; Koch and Friedrich 2012). Organic-rich Upper Cretaceous sequences in the south Lurestan zone were deposited in an extensive highly creative upwelling-linked system which prevaileda long the southern Tethys margin and lasted for Late Campanian (Fig. 9c and e). The nature of the upwelling system, and it's accomplished on the sedimentary record, is related to two basic environmental parameters, namely paleoproductivtiy strength and oxygen levels at the lower. Glauconite as well as phosphorite are associated with the Upper Cretaceous transgressive deposits of passive continental margins (Amorosi 2012). The phosphates developed during a period of transgression and onlap that promoted sediment starvation in a strata of limestones and greensands that were already defective in clastic supply. This upwelling system belongs to the Upper Cretaceous–Eocene phosphate belt which stretch from South America (Colombia) over North Africa to the Middle East be composed of organic-rich carbonates, cherts and phosphates (Pufahl et al. 2003, 2006).

Depositional environment

The Late Campanian and Maastrichtian care for the closing of the Southern Neo-Tethys and formations intraplate extensional and transextensional basin, in addition to the

deposition of the Seymareh Member in the Lurestan (Alavi 2004). The abduction and the closure of the Southern Neo-Tethys occurred during the Late Campanian and Maastrichtian, where the continental crusts of the Iranian and Arabian Plates were assemble (Alavi 2004). Because of this assembly, the studied area was transmuted from passive margin to active early Zagros foreland basin, and Seymareh Member in Gurpi Formation was deposited in this foreland basin. Particularly, we address Cretaceous submarine canyon evolution in South Lurestan Zone and links to sea-level vacillation (Fig. 7a and b). Large fragmented shells of *Lopha* Sp. *Pycnodonte* and echinoid, and foraminifers are in the whole succession in Seymareh Member. The diverse unormal marine macro-and microfossil that includes planktonic organisms and the muddy and sparity textures of the deposits suggest an open marine condition. A mixed benthic/pelagic microfossil association with a macrofossil by oysters, gastropods and echinoid debris describe the outer shelf microfacies (Flugel 2013). The intergranular space is satisfied with a micrite and sparite matrix. More internal benthic fauna can sometimes be met by chance and was probably brought in by storms. Gurpi Formation shallows upward to the microbioclast wackestone/packstone facies below the Seymareh Member with an abundance of benthic foraminifera, echinoid, oyster and bivalve shell fragments that reflect a distal outer-shelf depositional environment. The Seymareh facies is classified from bioclast wackestone to grainstone that contains a mixed benthic/pelagic microfossil association with a macrofossil by oysters and echinoids recommend as suitable that the Seymareh Member was deposited in a submarine canyon environment in the uppermost Campanian (Fig. 8a–d). High relative abundance of faunal substance of the Seymareh Member indicates oxygenated situations where circulation in the water body was strong and a shelf

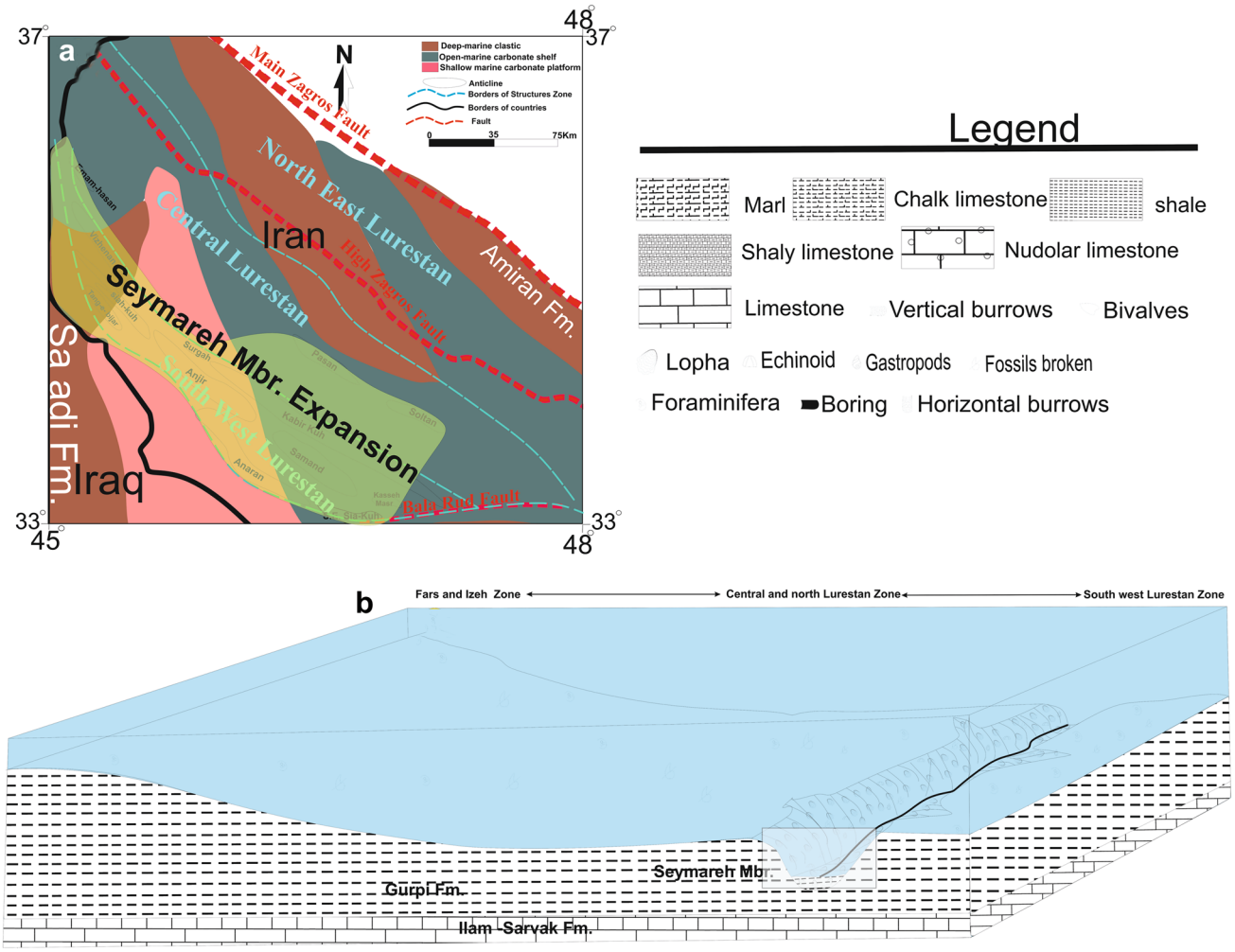

Fig. 7 **a** Paleogeographic map of Lurestan Zone during the late Campanian–Maastrichtian. Paleogeographic reconstruction showing simplified plate boundaries and Seymareh Member of Plate Arabian (with slightly modified after Ziegler 2001; Motiei 1995). **b** Schematic block diagram for depositional model of the Syemareh Member in Lurestan zone with available alchemy

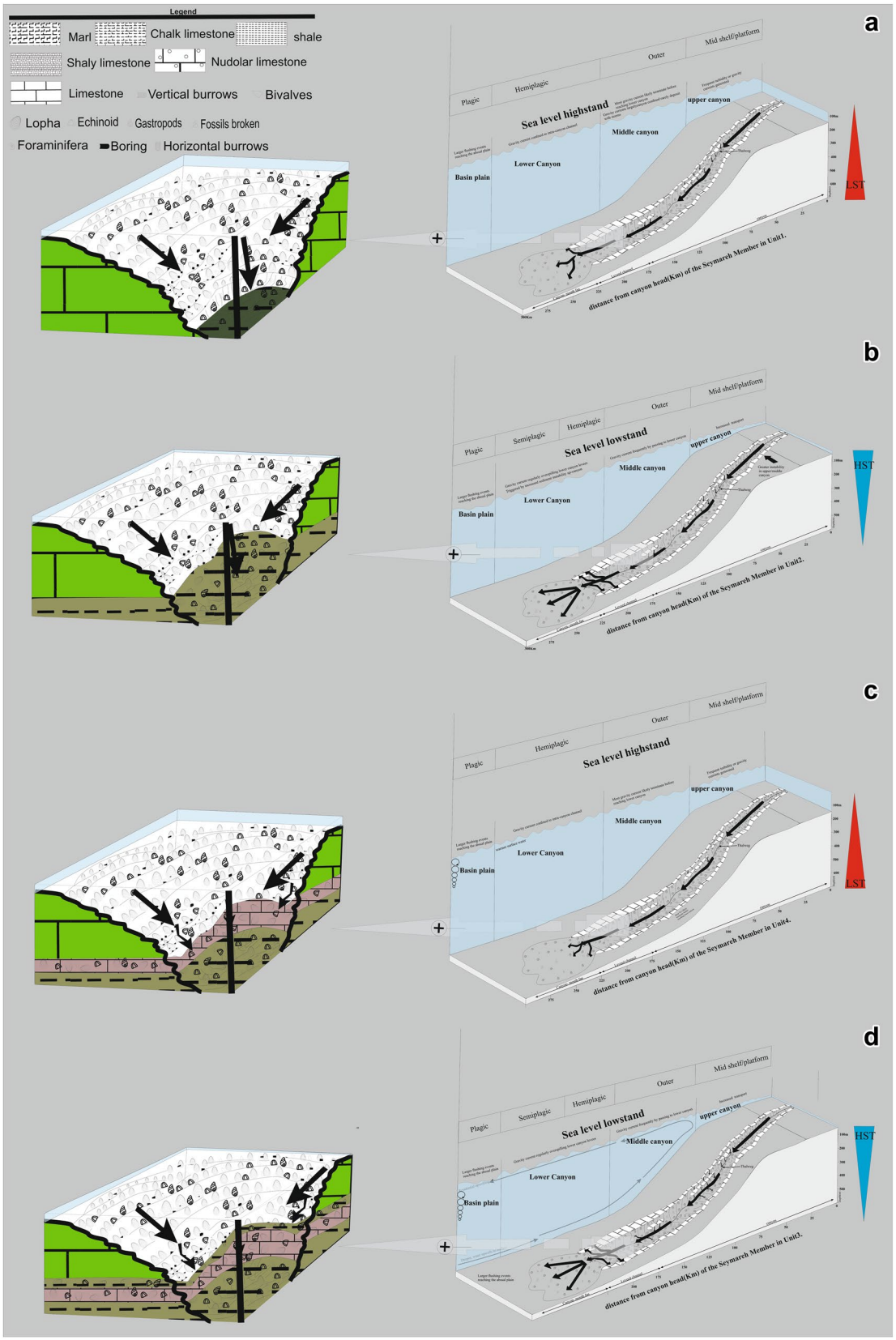

Fig. 8 **c** and **d** Schematic depositional models of the Seymareh Member during the highstand system and lowstand system in stratigraphic Unit 1 and 2, Close-up view of grey square of **b** and **c**. **e** and **f** Schematic depositional models of the Seymareh member during the highstand system and lowstand system tract in stratigraphic Unit 3 and 4, Close-up view of grey square of **d** and **e**

fauna dominated by the large *Lopha* sp. This is followed by a sudden decreasing and not moving condition and the deposition of pelagic wackestone microfacies. The high components of pyrite, glauconite and phosphates in organic microfacies are proof of surface water productivity and suboxic to the anoxic condition that favorite accumulation and protection of Seymareh Member in the pelagic environment in Late Campanian–Maastrichtian. Palaeoecologically, like their modern delegate, Campanian oysters lived near the foreland bulge and low-energy marine environments. In general, shell thickening among reclining species has almost definitely been a mechanism for expanding whole animal density to avert their being turned over and transported to undesirable habitats (Stanley 1970; Seilache 1984). However, some of the shells may have remained as encrusters in every part their life growing into substrates (such as shells) as evidenced. Moreover, the oyster populations in the present study are composed of different growth stages from youth to full-grown forms. The presence of youth and small individuals is probably due either to high youth mortality by flow in a high-energy marine environment (El-Ayyat and Kassab 2004). *Lopha* and *Pycnodonte* mostly populated warm and normal marine shallow to deep subtidal conditions and could have lived in deeper seas and additional away from the coasts (Dhondt et al. 2005; Wilson 2007). However, some of its ichnospecies are displayed in both deep and shallow water (Wilson 2007). Therefore, the global sea-level stand up at the Late Campanian-Early Maastrichtian boundary drowned the oyster habitats below their best water depth (Dhondt et al. 1999). During slow transgression, each *Lopha* sp. and other macrofossils will have adequate time to destroy the work of the previous one, and the resulting sculptures will reflect only the work of the deepest water community (Bromley and Asgaard 1993). The great incident of traces of oyester in the studied specimens shows approving conditions for their existence. There is the suggestion that at least parts of the Seymareh Member represent a transported fauna. Size differentiation of the individuals has been observed at unusual districts in all sections. Size differentiation is possibly the result of sorting by sedimentary processes. A transported organism oyster is formed when the smaller individuals of an assemblage are winnowed out and concentrated separately. In general, at the time of the deposition of the Gurpi Formation, the depth of the basin was from the south-east to the north-west of the Zagros Basin. Therefore, the deepest part of the Gurpi Formation Basin is connected to the Lurestan zone (Fig. 8a–d). There is Seymareh Member in the southern part of Lurestan zone, so Seymareh Member is deposited in the deep part of the Gurpi Formation Basin. According to the above, it appears that the Seymareh Member was deposited in a protected area in the deep marine (e.g.: Van Rooij et al. 2010). *Lopha* sp. and other macrofossils seem to grow in the submarine canyon wall and are then replaced by environmental factors. Generally, Submarine canyons are ubiquitous morphologic elements of global continental margins, serving as sediment transport conduits from shallow part marine to the deep sea, and as a key component in marine biologic productivity and biodiversity (Talling et al. 2015). The main driver for this ecosystem is a cautiously balanced hydrodynamic environment regulating sediment and nutrient supply (Dorschel et al. 2009; Amblas et al. 2018). Canyons play a judgmental role since they are the most important mechanism of nutrient input into the deep marine (Palanques et al. 2009). The morphology of the continental slope is described by canyons, arranged in channeling basins and actively feeding the Seymareh Member deep-sea fans (Anaran anticline). Despite this critical position, submarine canyon head deposits have accepted little containing details sequence stratigraphic study (e.g., Sweet and Blum 2016), in part because they are largely reasonable to locate of seascape humiliation and sediment avoid (e.g., Stevenson et al. 2015). The upper part of the paleocanyon unit contains comparatively small channels that were likely carved by erosion in all section and filled deposits. Canyon walls (Place of growth of the Lopha and other organism) were likely unstable and arrange to submarine landslide neglect because they consisted of relatively not unified Gurpi Formation shelf deposits and recently deposited canyon fill 9anjir and Emam-hasan anticlines). Within Canyons and trench, prevalently downslope erosion has progressively exposed these united carbonate-like sedimentary sequences, which have been shaped into step like banks or slope. This process is more intensive towards the centre of the canyon, providing a higher obtainability of appropriate substrates (Kabir-kuh sections). The overhanging banks and the perpendicular slope may provide an adequately protected habitat for the deep-water oysters. Moreover, the asymmetry of Seymareh Canyon clearly exhibits a second-factor control of the position of the deep-water oyster habitats. The lowest paleocanyon fill is commonly mixed microfacies with texture wackestone to grainstone, suggesting that mass transport deposits may be more common during the first stage of paleocanyon filling, shortly after incision when canyon alleviation may have been largest. Nested channel compounds within the paleocanyon unit are described by Facies Mf1 paleo-axial channel fill and lag deposits at the base of erosional channels and in pile combine units, overlain by Facies Mf2 and (or) Mf3. Facies Mf4 records canyon head deserting, resulting in finer-grained draping to downlapping fill. In Mf1 and Mf3 with slump folding depth of incision, channel location, and channel cross-sectional morphology indicate that much of the erosion and filling must have occurred below sea level, in a submarine- canyon environment (e.g., Fig. 7a and b). Conversely, the upper portion in Soltan, Pasan and Kase-mast anticline contains Mf1 and Mf4 incised by shallow, narrow

to amalgamated channels of Mf4 that may have been carved dominant. As a whole Seymareh Member is formed just southwest of Lurestan in a submarine canyon and little trace of this submarine canyon is seen as submarine dolines in the Sultan and Pasan anticline of central Lurestan. Due to the thickness and trend of the fossils it seems that the trend and slope direction of this canyon has been from the central Lurestan zone to the southeast of the southwestern Lurestan zone. So that in the Kabir-Kuh and Samand anticline most of the canyon wall (Ridge Lopha) in section Surgha and Anaran anticline was most likely to form fan canyon. It should be noted that the thickness of Seymareh Member differs from these anticlines in differentlocations, possibly due to tectonic conditions as well as the formation of subcanyons attached to the main canyon. This fact investigates the widespread of the same tectonic and environmental conditions with some time elapse along the border of the Arabian platform (Special in Lurestan Zone) in foreland bulge from Turkey to Iran (e.g., Alavi 2004). This time interval is entirely influenced by the compressional regime of the foreland basin creation (e.g., Alavi 2004; Homke et al. 2009), and Lopha limestone was probably deposited on the foreland bulge.

Sequence stratigraphy

Principal sequence stratigraphic conceptual models do not regard submarine canyon head settings in detail (e.g., Catuneanu et al. 2009, 2019). Although quantity sequence stratigraphic of concept models explain the bulk of submarine canyon fill to take place during sea-level transgression (e.g., Williams and Graham 2013), it is probably that some, or maybe most, of the observed Seymareh paleocanyon fill accumulated during long, slow regressions that controled Cretaceous sea-level cycles. We explain that some, and maybe main, of the sediment filling the paleocanyons was deposited during long, slow Cretaceous retrogression. Comparing Cretaceous sequence with the global sea-level curve of Haq et al. (1988) shows that this time interval is completely affected by the compacted regime of the foreland basin creation during the late Campanian-Maastrichtian sea-level lowstand that exposed the shelf in the south Lurestan zone, deposite Seymareh Member may have enlarged across the shelf and into Seymareh Canyon by way of flow canyon heads that abide as indentations along the northern rims of Canyon. It has also been suggested that climate-driven sea-level change can influence the frequency of canyon filling gravity or turbidity flow by impacting slope stability (Brothers et al. 2013). Upwelling connected with retrogression and lowstands may also have increased sediment supply (e.g., Evangelinos et al. 2017; Mauffrey et al. 2017). However, the reaction of sediment supply to Cretaceous climatic vacillation is still debated and may vary with regard to a certain location (e.g., Romans et al. 2016). We identified that a confusing interaction likely exists between eustatic sea-level, distance between the canyon head and sediment source(s), tectonics, and sediment supply (e.g., Mauffrey et al. 2017). The Seymareh paleocany on unit mentions that change sea level to canyon main distances and amount of sediment evade, largely due to shifts in canyon main location and sea-level variation. The Seymareh paleocanyon deposits record a mediatory step in sediment transport from tectonically uplifted the beginning of the canyon area to final submerges in the Seymareh deep-sea fan (Fig. 10a, b, c and b). The Seymareh Canyon has been elucidated to be working as a short-term reservoir for coarse sediment that is transported to the deep-sea fan in episodic events (e.g., Gontharet et al. 2007). In this section, we discuss the precipitate and controls on canyon-filling gravity currents or flow in Seymareh Canyon.

Highstand system tract (units 1 and 3)

The procedure of canyon-satiating occurs on a diversity of different transitory and spatial scales within Seymareh Canyon. Under the current proportionately high sea-level situations, the canyon head is mainly an area with deposition in the axial channel from sediment gravity flows that transport sediment into deeper water, and with the minor downfall of deposits along canyon walls apparently moved down canyon rapidly (e.g., Puig et al. 2014; Xu et al. 2014). Late studies of deep-water deposition along tectonically active margins exhibit that sediment transport and deep-sea fan deposition can take place or increase throughout transgression and sea-level highstand conditions where canyon leads abide joined to shore sediment (or shallow marine) transport systems (e.g., Gamberi et al. 2015; Sweet and Blum 2016) (Figs. 9 and 10c and e). However, these studies of highstand-dominated systems mainly depend on modern canyon morphology and concentrate on canyon heads as zones of sediment Seymareh Member. Where canyon heads keep pace with sediment deposition and protection should be tied to sea-level variation and sediment supply, and produce different sequence stratigraphic expression. These small and frequent gravity currents do not seem to deposit on canyon levees, or the abyssal plain, as there is a general absence of gravity deposited. Given the attendance of erosive scours within the lower obtain of the canyon, it is possible that these happening often gravity currents are erosive from for the upper to the lower canyon but are too small to rise above levees (de Stigter et al. 2002; Arzola et al. 2008). Upwelling has been HST and has led to high nutrients, thereby providing conditions for the growth of organisms as well as the formation of gluconate and phosphate in the canyon (Figs. 9 and 10c and e).

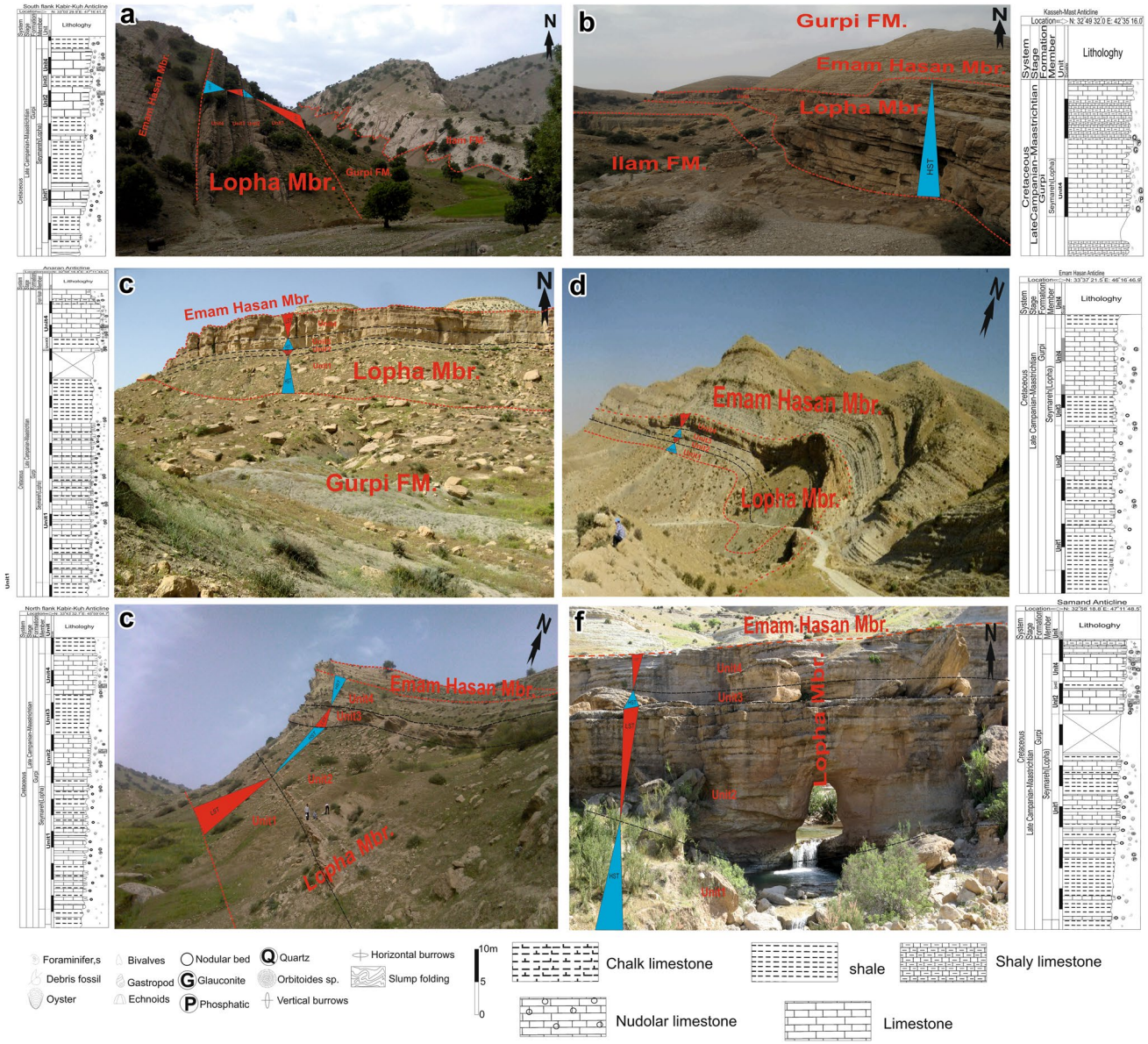

Fig. 9 Outcrop photograph and synthetic sedimentological log and system tract the Seymareh Member in the study area. **a** South flank Kabir-kuh section. **b** Kasse-Mast section. **c** Anaran section. **d** Emam-hasan section. **e** North flank Kabir-kuh section. **f** Samand section

Lowstand system tract (Units 2 and4)

We derive that many large-scale internal erosional surfaces shaped mainly during Cretaceous sea-level lowstands and regressions. In these models, submarine canyons are joined to terrestrial sediment furnish deposite Seymareh Member during lowstands, and are principally reasonable as bypass territory for sediments deposited in lowstand systems tract basin floor fans and wedges (e.g., Catuneanu et al. 2009; Catuneanu 2019). The role of sea-level lowstand in revealing continental shelves and resulting in more terrigenous sediment distribution to slope and deep-sea fans is widely approved; as is the role of canyons as a channel for this sediment delivery (Lebreiro et al. 2009). Lowstand dominated canyons typically occur when the canyon does not engrave the whole continental shelf (Covault and Graham 2010). In the lowstand system tract, internal erosional surfaces would depict sequence boundaries, and the wackestone and packstone textures paleocanyon fill would correlate with lowstand fan and lowstand wedge deposits farther toward the sea in deeper-water regions of the Channel and Fan (Fig. 9c and d). This results in a higher frequency of gravity currents due to increased sediment equip (Covault and Graham 2010). Despite the lack of a gravity sediment supply into Seymareh Canyon, there are a number of gravities for systems to the south Lurestan zone which feed onto the continental shelf

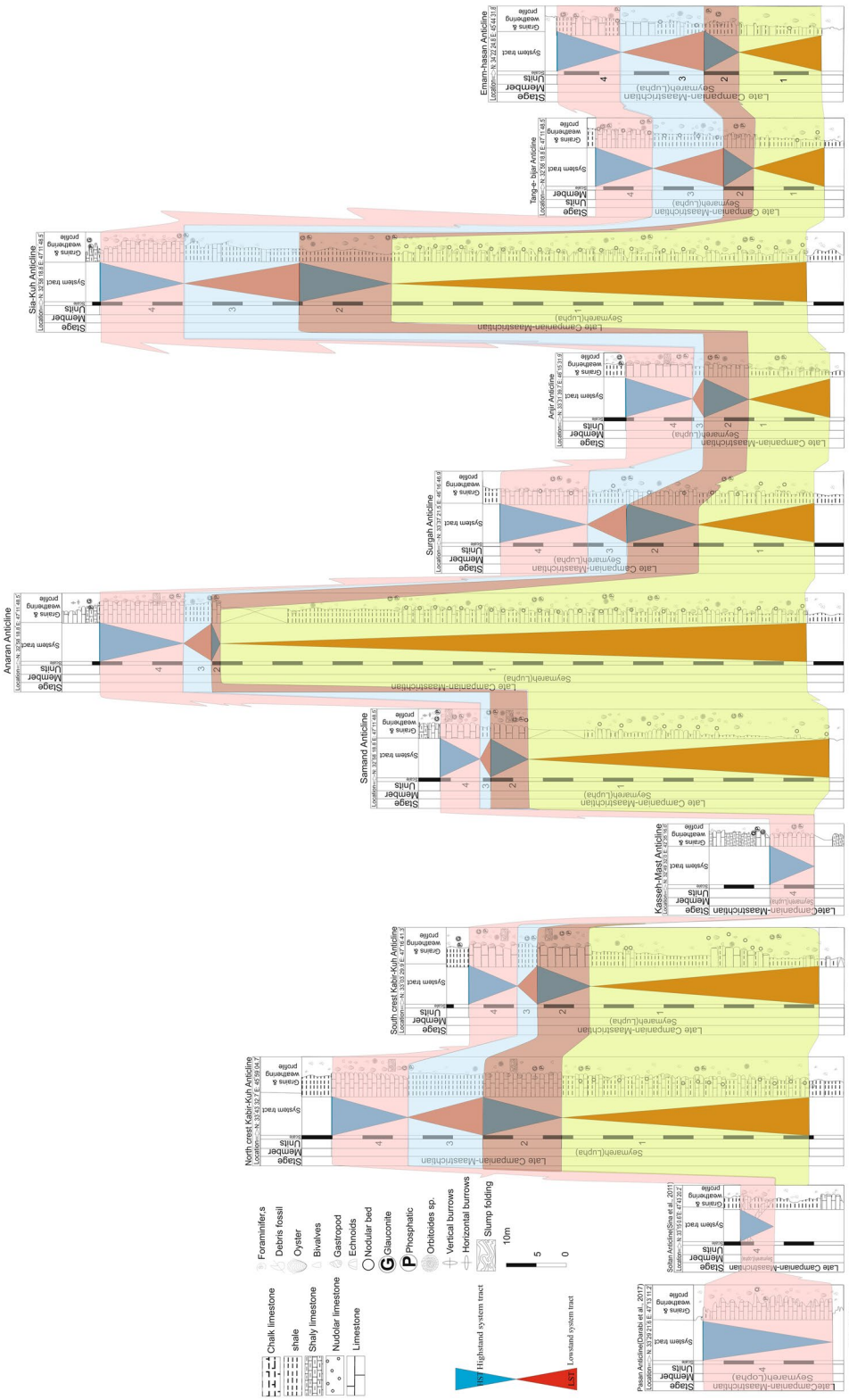

Fig. 10 Correlation of Sequence stratigraphy column, stratigraphic units and rock components of the Seymareh Member in the studied sections

(southeast toward southwest). Increased sediment compensates for to the shelf from these gravity currents during lowstand situations may also have led to increased sediment transport, and contributed to the higher frequency of gravity currents being produced. It is also might be that these gravities deposited were conquered across the shelf and into the canyon principal during sea-level lowstand. As the slope is converge with canyons, these tidally make happen transports may be channelled and result in domains of locally increased flow and local circulations (Pingree and Le Cann 1990). This is reminiscent of a margin-wide sea-level control on large-scale canyon-filling in Seymareh canyons. This is specifically true in the case of deep-water fan and continental slope settings in Surgah to Anaran sections. In these deep-water settings, one of the primary expressions of sea level changeability is replaced in down system sediment transport (Covault et al. 2010, 2011). For gravity currents, these can comprise the activate mechanism, sediment volume, run-out distance (Talling et al. 2013, 2015; Talling 2014). *Lopha* sp. and *Pycnodonte* are sequenced in different directions and in some layers are in the direction of flow indicating a submarine flow. The height of the wall above the canyon also likely prevents smaller, more frequent events triggered by storm or wave activity from depositing. This infer that if canyon-rinsing events are the result of climatic changeability (Bernhardt et al. 2015).

Conclusions

In throughout Cretaceous in Gurpi Formation of the south Lurestan Zone one deep-water ecological system hotspots have been recognized in association with a compound interplay of nourishing supply, sediment, geology and seabed morphology and this qualification was operative emersion Seymareh Member. The regional act of distinguishing most likely reflects their location on separate tectonic zones on which distinctive facies conditions matured due to different tectonic movements. This Seymareh Member is most uncommon with respect to its surroundings, geochemical signature, size and its especially significant centennial long life. More specifically, the area underneath overhanging cliffs and steep escarpments appear to be the most successful colonization surface. Only sometimes, and in reduced numbers, they can be found on exactly alike substrates colonized by the deep-water oysters. Such specific substrates can be considered as limited along the continental margins and are specifically gathered together into deep-sea canyons, where they still are comparatively sparsely scattered. The present observations exhibit that canyons and steep slopes may supply the most appropriate physical environment for these oysters (Lopha and other organisms), which are generally observed underneath overhanging banks or on escarpments. Seymareh Canyon head formation diverse inward Late Campanian sea-level oscillations, immigrate beyond the continental shelf in southwest Lurestan zone. Glauconites and phosphorite grains were authigenically precipitated within precursor marl and biosiliceous deposits during high water level and extreme upwelling within the Tethys Ocean to the east of Zagros Iran. In Seymareh member in rock units 2 and 4, the percentage of gluconite, P_2O_5, K_2O and Al_2O_3 is more than the other two rock units. The above evidence suggests an increase in water level and an increase in ambient energy, which seems to be the phenomenon of upwelling. The lower parts of paleocanyon fills include paleo-axial channel combined deposits and mass transport deposits from canyon wall failures; these and incision of paleocanyons may have taken place, or been improved, during retrogression and lowstands. Sea-level transgression and highstand likely promote sea-level oscillations and led to canyon head abandonment. This resulted in marine hemipelagic and gravity fill, possibly including paleo-bench deposits and spillover from the continental shelf, specifically in the upper part of the paleocanyon unit. A small portion of the uppermost paleocanyon unit includes channels, likely carved by extensions of the deposits Seymareh Member across the shelf during sea-level lowstands. The four upward cycles identified from the Seymareh are related to sea-level variations. Three complete 4rd-order depositional sequences in Deeping patterns were identified in the studied Member. The superior facies associations developed in member exhibit an overall transgression-regression cycle in the middle to late Campanian. Canyon-filling seems to be predominantly controlled by sediment unsteadiness during sea-level low stand and by storm during the present day highstand. Gravity currents are one of the main transport processes within Seymareh canyon systems and can be activated by a wide variety of mechanisms. Canyon-filling gravity currents are measured to be the result of made local sediment failures and storm resuspension. Canyon-flushing gravity currents are erosive flows that transport large volumes of this canyon-filling sediment out onto canyon-mouth fans.

Acknowledgements We gratefully appreciate the laboratory support supplied by the Department of Geology, Shahid Beheshti University, Shiraz University and Ferdowsi Mashhad University. We thank are Dr Ali hashmie and Saeid Afsarifard for insightful comments on earlier and final drafts of this manuscript and especially during field and laboratory work.

References

Ahmad F, Farouk S, El-Kahtany K, Al-Zubi H, Diabat A (2015) Late Cenomanian oysters from Egypt and Jordan. J Afr Earth Sc 109:283–295

Alavi M (2004) Regional stratigraphy of the Zagros fold-thrust belt of Iran and its proforeland evolution. Am J Sci 304(1):1–20
Amblas D, Ceramicola S, Gerber TP, Canals M, Chiocci FL, Dowdeswell JA, Lastras G (2018) Submarine canyons and gullies. Submarine geomorphology. Springer, pp 251–272
Amorosi A, Guidi R, Mas R, Falanga E (2012) Glaucony from the Cretaceous of the Sierra de Guadarrama (Central Spain) and its application in a sequence-stratigraphic context. Int J Earth Sci 101(2):415–427
Aqrabawi M (1993) Oyster (Bivalvia-Pteriomorphia) of Upper Cretaceous rocks of Jordan. Palaeontology, stratigraphy and comparison with the Upper Cretaceous oyster of Northwest Europe. Mitt Geol-Palaontol Inst Univ Hamburg 75:1–135
Arzola RG, Wynn RB, Lastras G, Masson DG, Weaver PP (2008) Sedimentary features and processes in the Nazaré and Setúbal submarine canyons, west Iberian margin. Mar Geol 250(1–2):64–88
Ayoub-Hannaa W, Fürsich FT (2011) Revision of Cenomanian-Turonian (Upper Cretaceous) gastropods from Egypt. Zitteliana 115–152
Bakhshandeh L, TehraniKh K, Mohtat T, Vaziri SH, Keshani F (2015) Biozonation of the Gurpi Formatin at Banroushan section, SW Ilam, based on Planktonic Foraminifera. Sci Q J Geosci 95:85–96 (**In Persian**)
Balmaki B, Babazadeh S, Vahidinia M, Asgharianrostami M (2010) Introducing of Echinoids of the Gurpi formation, Seimareh Member, Ilam province, Iran. Paper presented at the 1 International Applied Geological Congress.
Banerjee S, Bansal U, Pande K, Meena S (2016) Compositional variability of glauconites within the Upper Cretaceous Karai Shale Formation, Cauvery Basin, India: implications for evaluation of stratigraphic condensation. Sed Geol 331:12–29
Barrera E, Savin SM (1999) Evolution of late Campanian-Maastrichtian marine climates and oceans. Special Papers, Geological Society of America, pp 245–282
Beiranvand B, Ghasemi-Nejad E, Kamali MR (2013) Palynomorphs' response to sea-level fluctuations: a case study from Late Cretaceous-Paleocene, Gurpi Formation, SW Iran. J Geopersia 3:11–24
Bernhardt A, MelnickD J-M, Argandoña B, González J, Strecker MR (2015) Controls on submarine canyon activity during sea-level highstands: the Biobío canyon system offshore Chile. Geosphere 11(4):1226–1255
Blanc EP, Allen MB, Inger S, Hassani H (2003) Structural styles in the Zagros simple folded zone Iran. J Geol Soc 160(3):401–412
Bromley RG, Asgaard U (1993) Endolithic community replacement on a Pliocene rocky coast. Ichnos 2(2):93–116
Brothers DS, Uri S, Andrews BD, Chaytor JD, Twichell DC (2013) Geomorphic process fingerprints in submarine canyons. Mar Geol 337:53–66
Burst J (1958) Mineral heterogeneity in "glauconite" pellets. Am Mineral J Earth Planet Mater 43(5–6):481–497
Casini G, Gillespie P, Vergés J, Romaire I, Fernández N, Casciello E, Embry J-C (2011) Sub-seismic fractures in foreland fold and thrust belts: insight from the Lurestan Province, Zagros Mountains, and Iran. Pet Geosci 17(3):263–282
Catuneanu O (2019) Model-independent sequence stratigraphy. Earth-Sci Rev 188:312–388
Catuneanu O, Abreu V, Bhattacharya J, Blum M, Dalrymple R, Eriksson P, Gibling M (2009) Towards the standardization of sequence stratigraphy. Earth Sci Rev 92(1–2):1–33
Checa AG, Jiménez-Jiménez AP (2003) Evolutionary morphology of oblique ribs of bivalves. Palaeontology 46(4):709–724
Covault JA, Graham SA (2010) Submarine fans at all sea-level stands: tectono-morphologic and climatic controls on terrigenous sediment delivery to the deep sea. Geology 38(10):939–942
Covault JA, RomansB W, Fildani A, McGann M, Graham SA (2010) Rapid climatic signal propagation from source to sink in a southern California sediment-routing system. J Geol 118(3):247–259
Covault JA, Romans BW, Graham SA, Fildani A, Hilley GE (2011) Terrestrial source to deep-sea sink sediment budgets at high and low sea levels: Insights from tectonically active Southern California. Geology 39(7):619–622
Darabi G, Sadeghi A (2017) The Gurpi formation (upper Santonian–upper Maastrichtian, Marun oil field) biostratigraphy and paleoecology investigation. Geopersia 7(2):169–198
Darabi G, Moghaddam IM, Sadeghi A, Yusefi B (2017) Biostratigrapy and palaebathymetry of Gurpi formation in Anticlin Sultan. J Res Earth Sci 31:137–152 (**In Persian**)
Darabi G, Moghaddam IM, Sadeghi A, Yusefi B (2018) Planktonic foraminifera and sea-level changes in the upper Cretaceous of the Gurpi Formation, Lorestan basin, SW Iran. J Afr Earth Sc 138:201–218
Darvishzadeh A (2009) Geology of Iran: stratigraphy, tectonic, metamorphism, and magmatism. Amir Kabir, Tehran
Dhondt AV, Jaillard E (2005) Cretaceous bivalves from Ecuador and northern Peru. J S Am Earth Sci 19(3):325–342
Dhondt AV, Malchus N, Boumaza L, Jaillard E (1999) Cretaceous oysters from North Africa; origin and distribution. Bulletin De La Société Géologique De France 170(1):67–76
Dill Jafar Nejad AAM (2007) Palenology and palinostratigraphy of Gurpi Formation in Tang-e-Bijar section in the Ilam province. Master thesis, Faculty of Science, Shahid Beheshti University, p 144
Dorschel B, Wheeler AJ, Huvenne V, de Haas H (2009) Cold-water coral mounds in an erosive environmental setting: TOBI sidescan sonar data and ROV video footage from the northwest Porcupine Bank NE Atlantic. Mar Geol 264(3–4):218–229
El-Ayyat AM, Kassab AS (2004) Biostratinomy and facies analysis of the upper Cretaceous oyster storm shell beds of the Duwi formation, Qusseir District, Red Sea Region Egypt. J Afr Earth Sci 39(3–5):421–428
El-Sabbagh AM, El Hedeny MM (2016) A shell concentration of the middle Miocene Crassostrea gryphoides (Schlotheim, 1813) from Siwa oasis, Western Desert Egypt. J Afr Earth Sci 120:1–11
El-Sabbagh A, Mansour H, El-Hedeny M (2015) Taphonomy and paleoecology of Cenomanian oysters from the Musabaa Salama area, southwestern Sinai Egypt. Geosci J 19(4):655–679
Esmaeilbeig MR (2018) Biostratigraphy of the Gurpi Formation (Santonian–Maastrictian) by using Globotruncanidae, Zagros Mountains Iran. Carbonates Evaporites 33(1):133–142
Evangelinos D, Nelson CH, Escutia C, De Batist M, Khlystov O (2017) Late Quaternary climatic control of Lake Baikal (Russia) turbidite systems: Implications for turbidite systems worldwide. Geology 45(2):179–182
Farzipour-Saein A, Yassaghi A, Sherkati S, Koyi H (2009) Basin evolution of the Lurestan region in the Zagros fold-and-thrust belt Iran. J Petrol Geol 32(1):5–19
Flügel E (2013) Microfacies of carbonate rocks: analysis, interpretation and application. Springer Science & Business Media
Friedrich O, Norris RD, Erbacher J (2012) Evolution of middle to Late Cretaceous oceans—a 55 my record of Earth's temperature and carbon cycle. Geology 40(2):107–110
Gamberi F, Rovere M, Marani MP, Dykstra M (2015) Modern submarine canyon feeder-system and deep-sea fan growth in a tectonically active margin (northern Sicily). Geosphere 11(2):307–319
Geel T (2000) Recognition of stratigraphic sequences in carbonate platform and slope deposits: empirical models based on microfacies analysis of Palaeogene deposits in southeastern Spain. Palaeogeogr Palaeoclimatol Palaeoecol 155(3–4):211–238
Ghasemi-Nejad E, Hobbi MH, Schiøler P (2006) Dinoflagellate and foraminiferal biostratigraphy of the Gurpi Formation (upper

Santonian–upper Maastrichtian), Zagros Mountains Iran. Cretac Res 27(6):828–835
Gontharet S, Pierre C, Blanc-Valleron M-M, Rouchy J-M, Fouquet Y, Bayon G, Party TNS (2007) Nature and origin of diagenetic carbonate crusts and concretions from mud volcanoes and pockmarks of the Nile deep-sea fan (eastern Mediterranean Sea). Deep Sea Res Part II: Top Stud Oceanogr 54(11–13):1292–1311
Hadavi F, Rasa-Ezadi MM (2008) Nannostratigraphy of Gurpi Formation in Dare-Shahr section (SW Ilam). J Appl Geol 4:299–308
Hadavi F, Senemari S (2010) Calcareous nannofossils from the Gurpi Formation (Lower Santonian-Maastrichtian), faulted Zagros range, western Shiraz. Iran Stratigraphy and Geological Correlation 18(2):166–178
Hadavi F, Shokri, N (2010) Nanostratigraphy of the Gurpi Formation in Southern Ilam (Cover Section). Sedimentary Facies journal No. 2
Haq BU, Hardenbol J, Vail PR (1988) Mesozoic and Cenozoic chronostratigraphy and cycles of sea-level change
Hashmie A, Rashwan M, El Hedeny M, Sharyari S, Rahimi S, Mansour H (2020) Facies development, palaeoecology, and palaeoenvironment of the Seymareh (Lopha Limestone) Member of the Gurpi Formation (Upper Campanian), Lurestan Province SW Iran. Geol J 55:1–14
Hemmati-Nasab M, Ghasemi-Nejad E, Darvishzad B (2008) Paleobathymetry of the Gurpi Formation based on benthic and planktonic foraminifera in Southwestern Iran. J Sci Islam Rep Iran 34:157–173
Hessami K, Koyi HA, Talbot CJ, Tabasi H, Shabanian E (2001) Progressive unconformities within an evolving foreland fold–thrust belt, Zagros Mountains. J Geol Soc 158(6):969–981
Homke S, Vergés J, Serra-Kiel J, Bernaola G, Sharp I, Garcés M, Goodarzi MH (2009) Late Cretaceous-Paleocene formation of the proto–Zagros foreland basin, Lurestan Province, SW Iran. Geol Soc Am Bull 121(7–8):963–978
Hower WF, Brown W (1961) Large-scale laboratory investigation of sand consolidation techniques. J Petrol Technol 13(12):1221–1229
Hu X, Wagreich M, Yilmaz IO (2012) Marine rapid environmental/climatic change in the Cretaceous greenhouse world. Cretac Res 38:1–6
Jassim SZ, Goff JC (2006) Geology of Iraq, DOLIN, sro, distributed by Geological Society of London
Karim KH, Surdashy AM (2005) Tectonic and depositional history of Upper Cretaceous Tanjero Formation in Sulaimaniya area NE-Iraq. J Sulaimaniya Univ (JZS) 8:1–20
Koch MC, Friedrich O (2012) Campanian-Maastrichtian intermediate- to deep-water changes in the high latitudes: benthic foraminiferal evidence. Paleoceanography 27(2)
Lebreiro S, Voelker A, Vizcaino A, Abrantes F, Alt-Epping U, Jung S, Gràcia E (2009) Sediment instability on the Portuguese continental margin under abrupt glacial climate changes (last 60 kyr). Quatern Sci Rev 28(27–28):3211–3223
Mahanipour A, Najafpour A (2016) Calcareous nannofossil assemblages of the Late Campanian-Early Maastrichtian form Gurpi Formation (Dezful embayment, SW Iran): Evidence of a climate cooling event. Geopersia 6(1):129–148
Malchus N (1996) Palaeobiogeography of Cretaceous oysters (Bivalvia) in the western Tethys. Mitteilungen Aus Dem Geologisch-Paläontologischen Institut Der Universität Hamburg 77:165–181
Malchus N (1998) Aptian (Lower Cretaceous) rudist bivalves from NE Spain: taxonomic problems and preliminary results. Geobios 31:181–191
Mauffrey M-A, Urgeles R, Berné S, Canning J (2017) Development of submarine canyons after the Mid-Pleistocene transition on the Ebro margin, NW Mediterranean: the role of fluvial connections. Quat Sci Rev 158:77–93
Mekawy M (2013) Taphonomy of Aptian–Albian Beds in the Gebel Mistan, Maghara Area, Northern Sinai Egypt. J Earth Sci Clim Change 4(2):5
Moradi M (2010) Biostratigraphy and paleoecology of Gurpi Formation in Farhad Abad section in the west of Darreh-shahr. Master thesis, Faculty of Science, Tehran University, p 130
Motiei H (1993) Stratigraphy of Zagros. Treatise Geol Iran 60:151
Nairn A, Alsharhan A (1997) Sedimentary basins and petroleum geology of the Middle East. Elsevier
Najafpour A, Mahanipour A, Dastanpour M (2015) Calcareous nannofossil biostratigraphy of Late Campanian–Early Maastrichtian sediments in southwest Iran. Arab J Geosci 8(8):6037–6046
Odin GS, Matter A (1981) De glauconiarum origine. Sedimentology 28(5):611–641
Okan Y, Hoşgör I (2010) The coleoid cephalopod from the early Miocene of Eastern Mediterranean (Diyarbakır, Turkey).
Palanques A, Puig P, Latasa M, Scharek R (2009) Deep sediment transport induced by storms and dense shelf-water cascading in the northwestern Mediterranean basin. Deep Sea Res Part I 56(3):425–434
Pingree R, Le Cann B (1990) Structure, strength and seasonality of the slope currents in the Bay of Biscay region. J Mar Biol Assoc UK 70(4):857–885
Podobina VM, Kseneva TG (2005) Upper Cretaceous zonal stratigraphy of the West Siberian Plain based on foraminifera. Cretac Res 26(1):133–143
Pufahl PK, James NP (2006) Monospecific Pliocene oyster buildups, Murray Basin, South Australia: brackish water end member of the reef spectrum. Palaeogeogr Palaeoclimatol Palaeoecol 233(1–2):11–33
Pufahl PK, Grimm KA, Abed AM, Sadaqah RM (2003) Upper Cretaceous (Campanian) phosphorites in Jordan: implications for the formation of a south Tethyan phosphorite giant. Sed Geol 161(3–4):175–205
Puig P, Palanques A, Martín J (2014) Contemporary sediment-transport processes in submarine canyons. Ann Rev Mar Sci 6:53–77
Rabani R, Ghasemi-Nejad A, Amini A (2009) Palinostra - tigraphy and sequence stratigraphy of Gurpi Formation in valley Shahr section southeastern of Ilam. Iran J Geol 10:3–13
Rahimi S, Ashouri AR, Sadeghi A, Ghaderi A (2017) Biostratigraphy of the Gurpi Formation based on planktonic foraminifera with emphasis on the Cretaceous-Paleogene boundary in Jahangirabad section, Kabirkuh Anticline, SW Iran. Iran J Petrol Geol 14:93–110 (**In Persian**)
Rahimi S, Ashouri AR, Sadeghi A, Ghaderi A (2018) Biostratigraphy of the Gurpi Formation based on planktonic foraminifera with emphasis on the Cretaceous–Paleogene boundary in Gandab section, with correlation of type section, Kabirkuh Anticline SW Iran. Stratigr Sedimentol J 34:37–52 (**In Persian**)
Rahimi S, Ashouri AR, Sadeghi A, Ghaderi A (2020) Biostratigraphy of Campanian—Maastrichtian sequences and facies analysis in Anaran and Samand Anticlines Zagros Iran. Arab J Geosci 13:643
Razmjooei MJ, Thibault N, Kani A, Mahanipour A, Boussaha M, Korte C (2014) Coniacian-Maastrichtian calcareous nannofossil biostratigraphy and carbon-isotope stratigraphy in the Zagros Basin (Iran): consequences for the correlation of Late Cretaceous Stage Boundaries between the Tethyan and Boreal realms. Newsl Stratigr 47(2):183–209
Razmjooei MJ, Thibault N, Kani A, Dinares-Turell J, Puceat E, Shahriari S, Voigt S (2018) Integrated bio-and carbon-isotope stratigraphy of the Upper Cretaceous Gurpi Formation (Iran): a new reference for the eastern Tethys and its implications for large-scale correlation of stage boundaries. Cretac Res 91:312–340

Romans BW, Castelltort S, Covault JA, Fildani A, Walsh J (2016) Environmental signal propagation in sedimentary systems across timescales. Earth Sci Rev 153:7–29

Seilacher A (1984) Sedimentary structures tentatively attributed to seismic events. Mar Geol 55(1–2):1–12

Senemari S, Usefi MSM (2013) Evaluation of Cretaceous–Paleogene boundary based on calcareous nannofossils in section of Pol Dokhtar, Lorestan, southwestern Iran. Arab J Geosci 6(10):3615–3621

Sharyari S, Kani A, Amiri-Bakhtiyar H (2017) Biostratigraphy, Gurpi formation in Samand anticline (Lurestan Zone), based calcareous nannofossil. Stratigr Sedimentol J 33:37–60 (**In Persian**)

Sharyari S, Kani A, Amiri-Bakhtiyar H, Jamali AM (2018) Biostratigraphy, Gurpi formation in Anaran anticline (Lurestan Zone), based calcareous nannofossil. Res Sci Geol J 35:139–161 (**In Persian**)

Sherkati S, Molinaro M, de Lamotte DF, Letouzey J (2005) Detachment folding in the Central and Eastern Zagros fold-belt (Iran): salt mobility, multiple detachments and late basement control. J Struct Geol 27(9):1680–1696

Sina MA, Aghanabati A, Kani AL, Bahadori AR (2010) Biostratigraphy study of Gurpi Formation in Poldokhtar section (Kuh-Soltan anticline) based on calcareous nannofossils. J Earth Sci 79:183–188

Stanley SM (1970) Relation of shell form to life habits of the Bivalvia (Mollusca), vol 125. Geological Society of America

Stenzel HB (1971) Oysters. Treatise on invertebrate paleontology, Part N, Bivalvia 3, N953-N1224

Stevenson CJ, Jackson CA-L, Hodgson DM, Hubbard SM, Eggenhuisen JT (2015) Deep-water sediment bypass. J Sediment Res 85(9):1058–1081

Sweet ML, Blum MD (2016) Connections between fluvial to shallow marine environments and submarine canyons: implications for sediment transfer to deep water. J Sediment Res 86(10):1147–1162

Talling PJ (2014) On the triggers, resulting flow types and frequencies of subaqueous sediment density flows in different settings. Mar Geol 352:155–182

Talling PJ, Paull CK, Piper DJ (2013) How are subaqueous sediment density flows triggered, what is their internal structure and how does it evolve? Direct observations from monitoring of active flows. Earth Sci Rev 125:244–287

Talling PJ, Allin J, Armitage DA, Arnott RW, Cartigny MJ, Clare MA, Hansen E (2015) Key future directions for research on turbidity currents and their deposits. J Sediment Res 85(2):153–169

Van Rooij D, De Mol L, Le Guilloux E, Wisshak M, Huvenne V, Moeremans R, Henriet J-P (2010) Environmental setting of deep-water oysters in the Bay of Biscay. Deep Sea Res Part I 57(12):1561–1572

Wagner A, Benndorf J (2007) Climate-driven warming during spring destabilises a Daphnia population: a mechanistic food web approach. Oecologia 151(2):351–364

Williams TA, Graham SA (2013) Controls on forearc basin architecture from seismic and sequence stratigraphy of the Upper Cretaceous Great Valley Group, central Sacramento Basin California. Int Geol Rev 55(16):2030–2059

Wilson BM (2007) Igneous petrogenesis a global tectonic approach. Springer Science & Business Media

Xu J, Sequeiros OE, Noble MA (2014) Sediment concentrations, flow conditions, and downstream evolution of two turbidity currents, Monterey Canyon, USA. Deep Sea Res Part I 89:11–34

Zakhera M, El-Hedeny M, El-Sabbagh A, Al Farraj S (2017) Callovian–Oxfordian bivalves from central Saudi Arabia: systematic palaeontology and paleobiogeography. J Afr Earth Sc 130:60–75

Zarei E, Ghasemi-Nejad E (2014) Sedimentary and organic facies investigation of the Gurpi Formation (Campanian–Paleocene) in southwest of Zagros Iran. Arab J Geosci 7(10):4265–4278

Ziegler MA (2001) Late Permian to Holocene paleofacies evolution of the Arabian Plate and its hydrocarbon occurrences. GeoArabia 6(3):445–504